Brain Connectivity
© Mary Ann Liebert, Inc.
DOI: 10.1089/brain.2016.0456

Abnormal coupling between DMN and delta and beta band EEG in psychotic patients

Anja Baenninger[1,2], Vanessa A Palzes[3], Brian J Roach[3], Daniel H Mathalon[3,4] , Judith M Ford[3,4], Thomas Koenig[1,2]

Affiliations:

[1]Translational Research Center, University Hospital of Psychiatry, University of Bern, Switzerland

[2]Center for Cognition, Learning and Memory, University of Bern, Bern, Switzerland

[3]San Francisco VA Medical Center, San Francisco, CA, USA

[4]Department of Psychiatry, University of California San Francisco, CA, USA

Corresponding author:

Thomas Koenig, Translational Research Center, University Hospital of Psychiatry, University of Bern, Bolligenstrasse 111, 3000 Bern 60, Switzerland.

Email: thomas.koenig@puk.unibe.ch

Author contributions:

AB, JMF, TK, VAP wrote the manuscript; AB, VAP performed the measurements; AB, BJR, VAP, TK conceived and implemented experimental procedures and scripts for analyses; BJR, VAP and DHM critically revised the manuscript

Key words: psychosis, functional network integration, global field synchronization (GFS), EEG-informed fMRI analysis (or EEG-fMRI study), eyes-open (EO) resting state, delta and beta bands

Running title: EEG-fMRI during resting state in psychotic patients

This paper has been peer-reviewed and accepted for publication, but has yet to undergo copyediting and proof correction. The final published version may differ from this proof.

Abstract

Common-phase synchronization of neuronal oscillations is a mechanism by which distributed brain regions can be integrated into transiently stable networks. Based on the hypothesis that schizophrenia is characterized by deficits in functional integration within neuronal networks, this study aimed to explore whether psychotic patients exhibit differences in brain regions involved in integrative mechanisms. We report an EEG-informed fMRI analysis of eyes-open resting state data collected from patients and healthy controls at two study sites. Global field synchronization (GFS) was chosen as an EEG measure indicating common-phase synchronization across electrodes. Several brain clusters appeared to be coupled to GFS differently in patients and controls: Activation in brain areas belonging to the default mode network (DMN) were negatively associated to GFS delta (1 – 3.5Hz) and positively to GFS beta (13 – 30Hz) bands in patients, whereas controls showed an opposite pattern for both GFS frequency bands in those regions; activation in extrastriate visual cortex was inversely related to GFS alpha1 (8.5 – 10.5Hz) band in healthy controls, while patients had a tendency towards a positive relationship. Taken together, the GFS measure might be useful for detecting additional aspects of deficient functional network integration in psychosis.

1. Introduction

For the last decade, neuroimaging data have been accumulating to provide support for anatomical and functional disconnectivity in schizophrenia suggested by Friston and Frith (Friston and Frith 1995, Friston 1996, Friston 1998) (for comprehensive reviews see Stephan, Friston et al. 2009, Pettersson-Yeo, Allen et al. 2011). The term "disconnection" refers to a failure of functional integration within the brain, and "functional integration" refers to the interaction of functionally specialized systems (i.e., populations of neurons, cortical areas and sub-areas; Friston 2002). Functional integration is necessary to adaptively integrate sensorimotor information for perception and cognition (Friston 2002).

Studies of the human brain at rest increased dramatically after the discovery that anatomically separated, but functionally connected regions display a high level of correlated blood oxygen-level dependent (BOLD) signal activity during rest, in the absence of a task. A network of brain regions becomes co-active during rest and the assumption has been that it reflects focus on internal tasks such as daydreaming, imagining the future and reviewing the past (Greicius, Krasnow et al. 2003). As a result, it has been labeled the "default mode network" or DMN. We will use the term DMN here, while acknowledging that it reflects more than processes invoked during passive rest (Binder 2012).

Patients with schizophrenia have been reported to have both hyper- as well as hypo- connectivity within the DMN, and between nodes of the DMN with other cortical and subcortical regions (for reviews see Fornito, Zalesky et al. 2012, Whitfield-Gabrieli and Ford 2012). The deviations seen in schizophrenia during rest are paralleled by EEG and MEG studies showing increased amplitudes in lower delta, theta, and higher beta frequencies, with decreased amplitude in alpha frequency during rest (Boutros, Arfken et al. 2008, Galderisi, Mucci et al. 2009, Siekmeier and Stufflebeam 2010).

The simultaneous acquisition of EEG and fMRI provides a method to link these complementary neuroimaging methodologies. Consistent with alpha band amplitude reflecting a relaxed, alert "DMN-like" state, Jann et al (Jann, Kottlow et al. 2010) reported positive associations between DMN activity and alpha amplitude. Importantly, there is a negative relationship between both alpha power and amplitude and sensory

networks (Goldman, Stern et al. 2002, Laufs, Krakow et al. 2003, Mantini, Perrucci et al. 2007, Jann, Kottlow et al. 2010). Consistent with the suggestion that DMN reflects more than passive daydreaming and mind wandering (Binder 2012), beta band amplitude and power correlated positively with activity in the DMN and negatively with sensory networks (Mantini, Perrucci et al. 2007, Jann, Kottlow et al. 2010). In accordance with the fact that alpha band power depends on thalamic activity (e.g. de Munck, Goncalves et al. 2007, Tyvaert, Levan et al. 2008) and is dampened during visual tasks (e.g. Toscani, Marzi et al. 2010), there is a positive correlation between amplitude and power in the alpha band and the BOLD response in the thalamus, along with negative correlations between alpha and the BOLD response in executive and visual areas of the brain (e.g. Goldman, Stern et al. 2002, Laufs, Kleinschmidt et al. 2003, Laufs, Krakow et al. 2003, Moosmann, Ritter et al. 2003, Goncalves, de Munck et al. 2006, de Munck, Goncalves et al. 2007, Jann, Kottlow et al. 2010, Scheeringa, Petersson et al. 2012).

Individual alpha frequency (IAF) is defined as the individual center of gravity in frequency of EEG power across all channels within the alpha range of 8 to 13 Hz (Jann, Koenig et al. 2010). The IAF has been found to be associated with various cognitive features such as task performance or working memory (e.g.Klimesch 1997, Richard Clark, Veltmeyer et al. 2004). Using IAF, Jann et al. (2012) furthermore revealed a positive association between temporal IAF fluctuations and the DMN as well as left and right working memory networks (Jann, Federspiel et al. 2012). Thus, while there is a relationship between alpha power and DMN, it is not unique to either alpha or DMN.

It is unknown how spatially distributed brain areas are integrated into transiently stable neural networks, although studies on visual perception suggest integration is instantiated through common-phase synchronization of neurons across areas of the brain (Singer 1999, Singer 2001, Kottlow, Jann et al. 2012). In their review of the literature, Uhlhaas and Singer (2010) noted that schizophrenia was associated with reduced phase locking of beta and gamma band oscillations across electrodes or trials, especially in patients with more severe positive symptoms, such as hallucinations (Uhlhaas and Singer 2010). In resting state data, the relative amount of EEG activity that can be explained by phase-synchronous brain activity can be quantified in frequency domain using

Abnormal coupling between DMN and delta and beta band EEG activity in psychotic patients (doi: 10.1089/brain.2016.0456)
Brain Connectivity
This paper has been peer-reviewed and accepted for publication, but has yet to undergo copyediting and proof correction. The final published version may differ from this proof.

a measure called Global field synchronization (GFS). A GFS value of 1 indicates that at the given frequency, all brain processes observable to the EEG have a common phase, whereas a GFS value of 0 indicates the absence of any preferred phase across the entity of observable sources. In a study of medication naive, first episode patients with schizophrenia, GFS values in the theta band during rest were significantly decreased relative to healthy comparison subjects (Koenig et al., 2001). The authors argued that this finding of reduced functional connectivity in the theta frequency represents a loss of mutual interdependence of memory functions. Interestingly, another study linking alpha band GFS to fMRI-BOLD signal changes identified regions overlapping with the DMN (Jann et al., 2009). Here, we aimed to extend this important relationship between the EEG-based measure of GFS and fMRI-BOLD to understand psychosis in terms of abnormalities of integrative mechanisms that potentially underlie the formation of resting state networks (RSNs).

2. Materials and Methods

2.1 Participants

Data were collected at two sites: San Francisco Veterans Affairs Medical Center (SFVAMC) and University Hospital of Psychiatry and Psychotherapy of the University of Bern (PUK Bern), Switzerland.

At the SFVAMC, 20 patients with DSM-IV schizophrenia (N = 13 paranoid type (295.30), N = 4 disorganized type (295.10), N = 2 undifferentiated type (295.90), N = 1 residual type (295.60)) and 5 schizoaffective disorder (295.70; total N = 25), and 20 age- and gender-matched healthy comparison (HC) subjects were studied. At the PUK Bern, 17 psychotic patients and 17 age- and gender-matched HC were studied. 9 patients were diagnosed according to the ICD-10 with schizophrenia (N = 6 paranoid type (F20.0), N = 2 undifferentiated type (F20.3), and N = 1 catatonic type (F20.2)), and 8 patients with brief psychotic disorder (F23). Hereinafter all patients across sites are referred to as psychotic patients (PP).

At the SFVAMC, PP were referred by community outpatient clinicians, and both HC and PP, were recruited by advertisements and word-of-mouth. At the PUK Bern, PP were recruited at the hospital and HC via word-of-mouth.

At both sites, exclusion criteria for HC included having any past or current history of psychiatric and neurologic disorder, or a first-degree relative with a psychotic disorder. For both groups, exclusion criteria were any past significant medical or neurological illness, head injury resulting in loss of consciousness, or substance abuse in the past three months. Additionally, HC had no history of substance dependence (except caffeine or nicotine), while PP did not meet criteria for substance dependence within the past year. A trained research assistant, psychiatrist, or clinical psychologist conducted all interviews. Study procedures were approved by the University of California at San Francisco Institutional Review Board and SFVAMC as well as the local ethics committee of the canton of Bern, Switzerland (KEK no. 192/05) and all participants provided written informed consent. Clinical and demographic data are presented in table 1.

Table 1

2.2 Procedures

At the SFVAMC site, simultaneous EEG-fMRI data were acquired during rest. Participants were instructed to keep their eyes open (EO) and fixated on a white cross (+) in the center of a black screen for six minutes. An Avotec projector behind the scanner was used to project the stimulus on a screen attached inside of the magnet bore, and subjects viewed the screen through a mirror attached to the head coil.

At the PUK Bern, simultaneous EEG-fMRI data were also acquired during rest. Unlike the SFVAMC site, EEG data were also collected outside the scanner for later artifact removal (see section 2.3). Both inside and outside the scanner, participants alternated between two minutes of EO and two minutes eyes closed (EC). During EO inside the scanner, they were instructed to fixate on a white cross on a black screen. During EC, the screen was fully black. Starting with EO, both conditions alternated twice for two minutes each, resulting in eight minutes total time. Three white flashes indicated a switch between conditions. The flashes were not too bright to disturb subjects during EO, but bright enough to be noticed in the EC condition. None of the participants reported any discomfort during the measurement. Stimuli were presented via goggles (VisualStimDigital MR-compatible video goggles; Resonance Technology Inc., Northridge, CA, USA), with a visual angle of 60°, a resolution of 800x600 pixels and 60Hz refresh rate. To deliver stimulus material, E-Prime

(Version 2.0.10.553, Psychology Software Tools, INC.) was used.

At both sites, trained personnel rated the severity of psychotic symptoms using the Positive and Negative Syndrome Scale (PANSS; Kay, Fiszbein et al. 1987).

2.3 EEG and fMRI Data Acquisition and Preprocessing

As the EEG and fMRI acquisition and preprocessing steps were different, in this section we describe the procedures for each site. At the SFVAMC, continuous EEG data were collected from 31 standard scalp sites (Fp1, Fp2, F3, F4, C3, C4, P3, P4, O1, O2, F7, F8, T7, T8, P7, P8, Fz, FCz, Cz, Pz, FC1, FC2, CP1, CP2, FC5, FC6, CP5, CP6, POz, TP9, TP10) and another electrode was placed on the lower back to monitor electrocardiograms (ECG). At the Inselspital of Bern, Switzerland, a 92-channel cap was used and two additional channels each served the recording of the electrooculogram (EOG; below the eyes) and the electrocardiogram (ECG; below the clavicles). Both sites mounted the sintered Ag/AgCl ring electrodes in an MR compatible electrode cap from Brain Products (Gilching, Germany; input range: 16.3mV, resolution: 16 bit) according to the 10-10 system and with a sampling rate of 5 kHz. Electrode impedances below 10 kOhm were targeted at the SFVAMC and below 20 kOhm at the Inselspital Bern, while restricting full EEG preparation to one hour avoiding possible tiring of participants, especially patients (SFVAMC: across all subjects, 89.0% of all electrodes had impedances below 25 kOhm, 10% were higher than 30 kOhm and mean impedance was 15.5 kOhm; PUK Bern: across subjects, 88.6% of all electrodes had impedances below 25 kOhm, 7% were higher than 30 kOhm and mean impedance was 17.5 kOhm). The nonmagnetic EEG amplifiers were fixed behind the head coil and powered by a rechargeable power pack placed in the bore of the scanner and stabilized with sandbags. The subject's head was immobilized using cushions. EEG data were transmitted via an MR-compatible fiber optic cable to a BrainAmp USB Adapter that synchronized the EEG acquisition clock to the MRI master clock via a SyncBox (Brain Products) before transferring data via USB to a laptop computer placed outside the scanner room.

To provide a better overview of EEG and fMRI acquisition parameters and preprocessing steps for each site, we assembled the information in table 2 (for a detailed EEG preprocessing description see supplemental

materials). Both sites used Brain Vision Analyzer (Version 2.0.4.368, Brain Products, Gilching, Germany) for the preprocessing of the EEG data and SPM8 for the processing of the fMRI data (SPM8; Welcome Department of Imaging Neuroscience, London, http://www.fil.ion.ucl.ac.uk/spm). The SFVAMC additionally had EEG analyses performed in Matlab (Mathworks, Natick, MA). Mean motion for each subject for each condition was computed as the root-mean-square of the translation parameters extracted from the fMRI data (Van Dijk, Sabuncu et al. 2012).

Table 2

2.4 Global field synchronization (GFS) of EEG

To adjust analysis parameters between sites (SFVAMC and PUK Bern), the EEG montage of Bern was reduced from 92 channels to the same 31-channels as used by the SFVAMC site (see section 2.3 above). The GFS values of the Bern data with 92 versus 31 channels were highly correlated (HC mean Pearson r = 0.96, SD = 0.019; PP r = 0.95, SD = 0.05). Consequently, we would not expect different results if we would have used all 92 channels of the Bern dataset. The procedures for the computation of GFS are described in previous papers from the PUK Bern (Koenig, Lehmann et al. 2001, Jann, Dierks et al. 2009, Kottlow, Jann et al. 2012) and briefly described as follows: For each subject, EEG data were segmented into 2-second-epochs in relation to the scan markers of each volume (SFVAMC: TR = 2 s, segmentation onset = 0, length = 2 s, total of 181 segments; PUK Bern: TR = 1.96 s, segmentation onset = -0.048, length = 2.048, total of 249 segments). Then, each epoch was frequency transformed using a complex Fast Fourier Transformation (FFT; maximum resolution = 0.48828Hz, zero-padding). The retained sine and cosine values for each electrode and frequency bin could be visualized in a two-dimensional sine-cosine diagram with one point for each electrode at a given frequency. The resulting shape of clouds of all electrodes is an indicator of the amount of zero-lag phase synchronization across electrodes. More specifically, if the cloud is nearly circular, no predominant phase angle is present in the EEG, as opposed to an elongated cloud adverting a common phase across electrodes. The quantification of the shape is done by means of a two-dimensional principal component analysis (PCA): GFS is then defined as the ratio of (E1-E2) to (E1+E2) of the two eigenvalues (E1 and E2; see formula 1), with values ranging from 0 (absence of

a common phase angle, minimal synchronization) to 1 (maximal phase synchronization; Koenig, Lehmann et al. 2001). For further analyses, the GFS values were averaged across epochs and frequencies for delta (1 – 3.5Hz), theta (4 – 7.5Hz), alpha1 (8.5 – 10.5Hz), alpha2 (10.5 – 12.5Hz), and beta (13 – 30Hz) band per subject.

Formula 1

2.5 EEG-informed fMRI analysis

To explore the anatomical correlates of GFS at different frequency bands (delta, theta, alpha1, alpha2, and beta) between groups, centered GFS values were used as parametric modulators for first-level fMRI analyses in SPM (SPM8; Welcome Department of Imaging Neuroscience, London, http://www.fil.ion.ucl.ac.uk/spm) using in-house Matlab scripts (Mathworks, Natick, MA) that removed the serial orthogonalization default setting in SPM (Wood, Nuerk et al. 2008). Serial orthogonalization was disabled because within subjects the different GFS frequency bands were not highly correlated with each other (overall mean Pearson r = 0.0532, min = 0.0211, max = 0.0828). First level analyses were run separately for SFVAMC and PUK Bern sites due to differences in the resting state acquisitions. We included the six motion parameters resulting from the realignment of the fMRI data (see fMRI preprocessing in table 2) as covariates of no interest into the design matrix of the general linear model to attenuate the variance induced by motion of each subject (Lund, Norgaard et al. 2005, Johnstone, Ores Walsh et al. 2006). In order to exclude bad intervals previously flagged in the EEG data, GFS values were set to zero (SFVAMC: Mean = 5.7, SD = 2.4 of 181 total trials, PUK Bern: Mean = 60.5, SD = 38.8 of 249 total trials; for EO trials: Mean = 25.5, SD = 15.5 of 123 total trials; for different approaches at each site see table 2) and values were centered at each frequency band to get the variance of the GFS predicting BOLD fluctuations. For the second-level analysis, only EO GFS-modulated betas were considered for the comparison of groups across both sites. To evaluate possible differences, the measuring site (SFVAMC, PUK Bern) was included in the statistical model as a covariate for the within- and between-group analyses.

Our analysis strategy was to explore EEG-fMRI coupled clusters that showed between-group differences first, and then within-group effects. Our initial voxelwise, cluster-finding threshold was set to p = 0.01 (two-sided).

3 Results

3.1 EEG-informed fMRI analysis – 2nd level results – Group differences

The EEG-informed fMRI analysis revealed brain clusters that were coupled significantly differently in the two groups for three of the five GFS frequencies, namely in the delta (1 – 3.5Hz), alpha1 (8.5 – 10.5Hz), and beta (13 – 30Hz) band.

3.1.1 Delta Band

In the delta band, there were seven clusters that differed between groups (cluster 1: 5506 voxels, FWE p = < 0.001; cluster 2: 1762 voxels, FWE p = < 0.001; cluster 3: 1420 voxels, FWE p = < 0.001; cluster 4: 308 voxels, FWE p = 0.004; cluster 5: 293 voxels, FWE p = 0.006; cluster 6: 232 voxels, FWE p = 0.022; cluster 7: 220 voxels, FWE p = 0.029; figure 1). Some clusters included regions of the default mode network (DMN), like the precuneus, the posterior cingulate gyrus and the inferior parietal lobule. Other clusters included temporal, parietal, thalamic, cerebellar and limbic regions (for details of regions see supplemental materials, table 1). Looking at the mean beta weights extracted from the between-group clusters for each group, all clusters had negative weights in patients and positive weights in controls (figure 2). Within group analyses revealed two significant positive clusters in healthy controls and eight significant negative clusters in patients (figure 1).

Figure 1

Figure 2

3.1.2 Alpha1 Band

In the alpha1 band, there was one cluster containing 434 voxels (FWE p = 0.004) that differed between groups in left hemispheric occipital, temporal and parietal areas such as the cuneus, precuneus, and Brodmann areas 7, 18, 19, 31 (see figure 3; for details of involved regions see supplemental materials table 1). Within the controls, there were two significant negative clusters overlapping with the cluster of the between-group contrast (figure 3). The mean beta weights revealed that controls showed negative, and patients positive associations explaining the group difference (figure 4).

Figure 3

Figure 4

3.1.3 Beta Band

In the beta band, there was one 252-voxel cluster (FWE p = 0.0026), located mainly in the right hemispheric precuneus and cuneus that differed between groups (see figure 5; for details of regions see table 1 in supplemental materials). The mean beta weights of that cluster revealed that this difference was explained by patients showing positive GFS beta – BOLD associations, while healthy controls had a negative coupling in that cluster (figure 6).

Figure 5

Figure 6

3.2 Follow up analysis – Influence of power across all channels in significant GFS group clusters

To elucidate how the measure of GFS was related to amplitudes of the corresponding frequency bands, in follow-up analyses, we ran similar first- and second-level analyses, but used mean power across all channels, instead of synchrony (GFS), as parametric modulators. First, the mean power in the three frequency bands, which showed significant group effects in the GFS analysis (delta, alpha1, and beta), was calculated. Mean power and GFS measures within each frequency band were not correlated with each other (overall mean Pearson r = 0.2463, min = 0.0666, max = 0.4814), so we were able to include both as parametric modulators in the same first-level model. In the end, we conducted three separate models, one for each frequency band. There were no overlapping voxels (initial threshold p = 0.01, two-sided; cluster size: 5) for GFS and global power for any of the frequency bands (delta, alpha1, and beta), indicating that these measures indeed capture different aspects of brain function. In addition, there were no significant clusters for global power surviving at the same initial height threshold as used in the main GFS analyses, so these data are not discussed further.

3.3 Differences in GFS frequencies between sites

We performed an ANOVA (5 × 2 factorial design with factors GFS frequency and site) and an additional independent samples t-test for all GFS frequencies (delta, theta, alpha1, alpha2, beta) to check for significant differences between sites (SFVAMC versus PUK Bern). There was a significant main effect of site ($p \leq .001$) resulting from the ANOVA and the t-test revealed additionally that each frequency band was significantly different between sites (all p-values ≤ .001): GFS values were always higher at the SFVAMC compared to the PUK Bern. The Levene's test for equality of variance resulting from the t-test indicated that there was no significant difference in the variance between sites in any of the GFS frequency bands (all p-values ≥ .070).

However, the results of the first-level analyses are mathematically independent of these differences between sites. In addition, this factor was included as covariate into the model for the second-level analysis. The finding may be due to different protocols at the two sites: subjects at the PUK Bern alternated between two-minute periods of EC and EO while subjects at SFVAMC had one six-minute period of EO.

3.4 Relationship between symptoms and brain clusters

We ran ANCOVAs, with site as a covariate, to explore systematic relationships of symptom severity as measured by total scores of positive, negative and general symptoms from the PANSS in PP on the mean EO GFS-modulator beta weights of the significant between-group brain clusters from the delta, alpha1 and beta bands. None of these tests reached significance (all $p > 0.05$, uncorrected).

3.5 Relationship between movement parameters and brain clusters

Because patients showed significantly larger mean head displacements than healthy controls (see table 1), we tested the relationship between the mean EO GFS-modulator beta weights of the significant brain clusters including the mean motion parameters as covariate of no interest. The group differences for each brain cluster were still highly significant when controlling for mean head displacements (all p-values < 0.001), thus our between-group results cannot be explained by group differences in head movement.

4 Discussion

Abnormal coupling between DMN and delta and beta band EEG activity in psychotic patients (doi: 10.1089/brain.2016.0456)
Brain Connectivity

The goals of this study were three-fold: To provide further evidence of a relationship between fluctuations in global common-phase neural oscillations and fluctuations in the BOLD response during rest, to determine the relationship between neural activity in specific frequency bands and BOLD activity in specific brain regions, and to ask how this relationship is affected by psychosis. Our EEG-informed fMRI analysis using the GFS values pooled into five frequency bands (delta, theta, alpha1, alpha2, and beta) revealed significant brain clusters that differed between groups in the delta, alpha1, and beta band.

4.1 Delta Band

The results in the delta band were the most extensive. They revealed seven clusters, including regions of the well-known default mode network (DMN): the precuneus, the posterior cingulate gyrus and the inferior parietal lobule. The results were driven by a negative relationship between GFS delta and regions of the DMN in the patients. The healthy controls had positive associations, but only with the right inferior parietal sulcus (rIPS) of the DMN. That is, when neuronal oscillations in the delta band were synchronized across the scalp, the DMN was *less* active in patients and *more* active in the healthy controls. Slow EEG oscillations have been linked to inhibitory processes of the brain (Contreras and Steriade 1995) and reduced states of alertness, such as drowsiness, sleep or sedation (Hlinka, Alexakis et al. 2010). Our results suggest that in psychotic patients, coordinated neuronal oscillations in the slow delta frequency are coupled with inhibited activity in the DMN. Synchronized delta activity might underlie known alterations of DMN connectivity as well as psychopathology in this patient population. Interestingly, the most preponderant abnormalities in quantitative EEG in psychotic patients are also found in slow rhythms (Boutros, Arfken et al. 2008, Galderisi, Mucci et al. 2009, Siekmeier and Stufflebeam 2010). Our findings may point to a missing link between the extensive literature on fMRI related DMN abnormalities and the equally well-replicated findings of increased slow EEG activity. Nevertheless, because both increased and decreased connectivity of the DMN are reported, the precise nature of the relationship between connectivity within the DMN and common-phase delta synchronization should be further investigated across rest and a variety of tasks.

4.2 Alpha1 Band

There was one cluster including extrastriate visual cortex showing a negative coupling between alpha1 in healthy controls, whereas no such modulation was seen in patients, resulting in the between-group effect. That is, in healthy controls but not patients, greater synchrony in the alpha1 band was related to less activity in visual cortex. Others have reported a negative relationship between alpha power and occipital brain activity, which has been discussed in terms of "idling" of the brain (Goldman, Stern et al. 2002, Laufs, Kleinschmidt et al. 2003, Laufs, Krakow et al. 2003, Moosmann, Ritter et al. 2003, Goncalves, de Munck et al. 2006, de Munck, Goncalves et al. 2007, Tyvaert, Levan et al. 2008, Jann, Dierks et al. 2009, Jann, Kottlow et al. 2010). Using the same measure of synchronization and definition of lower and upper alpha band that we used, Jann et al (2009) reported a positive relationship between GFS in lower alpha (8.5 – 10.5Hz) and the BOLD signal in brain areas corresponding to the dorsal attention network (dAN), whereas GFS in upper alpha (10.5 – 12.5Hz) was positively correlated to the DMN (Jann, Dierks et al. 2009) in healthy subjects. While the procedures of integrating the alpha band GFS with the fMRI BOLD data were similar, in our healthy controls, we did not see a relationship between GFS alpha1 and the dAN reported by Jann et al (2009). This might be explained by some important differences between the studies: First, in our study, subjects had their eyes open, whereas in Jann et al., eyes were closed. Second, the subjects in the Jann et al study were about 10 years younger than the healthy controls in our study.

4.3 Beta Band

The between-group effect found in the right precuneus due to patients displaying a positive coupling between GFS in the beta band and activity in the precuneus, with healthy controls showing negative association. The precuneus, a "hub" region of the DMN, is engaged in visuospatial imagery, episodic memory, reflective, self-related processing, awareness and conscious information processing (Cavanna and Trimble 2006, Zhang and Li 2012). As oscillations in the beta frequency range have been associated with polymodal sensory processing, sensory-motor coordination, the maintenance of limb positions, and working memory (Uhlhaas, Haenschel et al. 2008), the positive association between beta GFS and DMN activity in patients may reflect an imbalance between perception/cognition and mind wandering. Findings of decreased induced and evoked beta

phase synchronization in circumscribed brain regions were positively correlated with positive symptoms (Uhlhaas and Singer 2010, Uhlhaas 2011), whereas deficits in the perception of Mooney faces in patients coincided with a reduction in global beta phase synchronization, suggesting impairment of large-scale synchronization (Uhlhaas and Singer 2006).

4.4 Conclusion

The associations between BOLD and global common-phase synchronization in low frequency delta, and also the higher frequencies in alpha1 and beta band, were altered in a variety of brain areas in psychotic patients, specifically in extrastriate visual areas for the alpha1 and DMN regions for the delta and beta frequency oscillations. The finding that patients and controls showed opposite patterns in their associations between GFS delta and beta band and the DMN, possibly reflects alterations in functional coupling between different nodes of the DMN. Not only regarding EEG, but also fMRI BOLD data, it was shown that different frequency ranges are related to specific brain regions (Gohel and Biswal 2015), and also that global changes of the BOLD signal should be captured too, as displayed by changes in psychotic patients (Hahamy, Calhoun et al. 2014).

The reported results in this study reveal novel aspects of the deficient functional integration in psychotic patients suggested by Friston (2002). We argue that by using concurrent EEG and fMRI, links between psychopathology and physiological measures of network integration on different time scales can be established. This may provide a more extensive understanding of psychosis and other serious mental illnesses.

4.5 Limitations

The possible influence of antipsychotic medications on the neurobiological data always limits the interpretation of results, and it is not common practice to withdraw patients from medications for scientific studies. Although it is difficult to disentangle the effects of medication from the reasons a particular dose of medication was prescribed, we found no statistically significant relationship between chlorpromazine equivalents and the mean beta weights of the significant group clusters. Despite growing evidence that the EEG gamma band is affected in psychosis (e.g. Uhlhaas and Singer 2006, Uhlhaas and Singer 2010, McNally and

McCarley 2016), its investigation in EEG-fMRI studies is limited: amplifier gain settings required to remove MRI gradient artifacts restrict us from measuring small amplitude (i.e., < 0.5 μV) signals like gamma band activity and the noisy environment (e.g., compressor pumps) may contaminate higher frequency bands in particular.

It is difficult for us to compare our findings to others in the literature, as there are few similar studies. This may be for several reasons: First, there are many different methods used to combine neural signals derived from simultaneous EEG and fMRI measurements. Second, most studies that looked for relationships between EEG and fMRI used spectral amplitude of the EEG signal. Third, only two studies (studying healthy subjects only) used a common-phase synchronization measure, and it was sensitive to a different aspect of neuronal oscillatory activation (Jann, Dierks et al. 2009, Kottlow, Jann et al. 2012). Fourth, most studies used EC during the resting state, while our subjects had their EO, which are two conditions associated with different mental states. The study of Wu and colleagues found that during EC, there were widespread alpha hemodynamic responses and high functional connectivity, whereas during EO these effects were markedly diminished (Wu, Eichele et al. 2010).

Acknowledgements:

We would like to thank all the participants that participated in our studies. Special thanks goes to Laura Diaz Hernandez and Kathryn Rieger for helping with the measurements. Andrea Federspiel and Kay Jann for MR-related questions. Nadja Razavi for her help regarding clinical-diagnostic interviews and Ulrich Raub for managing the recruitment process.

Author Disclosure Statement:

All authors hereby declare that there is no actual or potential conflict of interest including financial, personal or other relationships with other people or organizations, which would inappropriately influence our work.

5 References

Binder, J. R. (2012). "Task-induced deactivation and the "resting" state." Neuroimage **62**(2): 1086-1091.

Boutros, N. N., C. Arfken, S. Galderisi, J. Warrick, G. Pratt and W. Iacono (2008). "The status of spectral EEG abnormality as a diagnostic test for schizophrenia." Schizophr Res **99**(1-3): 225-237.

Cavanna, A. E. and M. R. Trimble (2006). "The precuneus: a review of its functional anatomy and behavioural correlates." Brain **129**(Pt 3): 564-583.

Contreras, D. and M. Steriade (1995). "Cellular basis of EEG slow rhythms: a study of dynamic corticothalamic relationships." J Neurosci **15**(1 Pt 2): 604-622.

de Munck, J. C., S. I. Goncalves, L. Huijboom, J. P. Kuijer, P. J. Pouwels, R. M. Heethaar and F. H. Lopes da Silva (2007). "The hemodynamic response of the alpha rhythm: an EEG/fMRI study." Neuroimage **35**(3): 1142-1151.

Fornito, A., A. Zalesky, C. Pantelis and E. T. Bullmore (2012). "Schizophrenia, neuroimaging and connectomics." Neuroimage **62**(4): 2296-2314.

Friston, K. J. (1996). "Theoretical neurobiology and schizophrenia." Br Med Bull **52**(3): 644-655.

Friston, K. J. (1998). "The disconnection hypothesis." Schizophr Res **30**(2): 115-125.

Friston, K. J. (2002). "Dysfunctional connectivity in schizophrenia." World Psychiatry **1**(2): 66-71.

Friston, K. J. and C. D. Frith (1995). "Schizophrenia: a disconnection syndrome?" Clin Neurosci **3**(2): 89-97.

Galderisi, S., A. Mucci, U. Volpe and N. Boutros (2009). "Evidence-based medicine and electrophysiology in schizophrenia." Clin EEG Neurosci **40**(2): 62-77.

Gohel, S. R. and B. B. Biswal (2015). "Functional integration between brain regions at rest occurs in multiple-frequency bands." Brain Connect **5**(1): 23-34.

Goldman, R. I., J. M. Stern, J. Engel, Jr. and M. S. Cohen (2002). "Simultaneous EEG and fMRI of the alpha rhythm." Neuroreport **13**(18): 2487-2492.

Goncalves, S. I., J. C. de Munck, P. J. Pouwels, R. Schoonhoven, J. P. Kuijer, N. M. Maurits, J. M. Hoogduin, E. J. Van Someren, R. M. Heethaar and F. H. Lopes da Silva (2006). "Correlating the alpha rhythm to BOLD using simultaneous EEG/fMRI: inter-subject variability." Neuroimage **30**(1): 203-213.

Greicius, M. D., B. Krasnow, A. L. Reiss and V. Menon (2003). "Functional connectivity in the resting brain: a network analysis of the default mode hypothesis." Proc Natl Acad Sci U S A **100**(1): 253-258.

Hahamy, A., V. Calhoun, G. Pearlson, M. Harel, N. Stern, F. Attar, R. Malach and R. Salomon (2014). "Save the global: global signal connectivity as a tool for studying clinical populations with functional magnetic resonance imaging." Brain Connect **4**(6): 395-403.

Hlinka, J., C. Alexakis, A. Diukova, P. F. Liddle and D. P. Auer (2010). "Slow EEG pattern predicts reduced intrinsic functional connectivity in the default mode network: an inter-subject analysis." Neuroimage **53**(1): 239-246.

Jann, K., T. Dierks, C. Boesch, M. Kottlow, W. Strik and T. Koenig (2009). "BOLD correlates of EEG alpha phase-locking and the fMRI default mode network." Neuroimage **45**(3): 903-916.

Jann, K., A. Federspiel, S. Giezendanner, J. Andreotti, M. Kottlow, T. Dierks and T. Koenig (2012). "Linking brain connectivity across different time scales with electroencephalogram, functional magnetic resonance imaging, and diffusion tensor imaging." Brain Connect **2**(1): 11-20.

Jann, K., T. Koenig, T. Dierks, C. Boesch and A. Federspiel (2010). "Association of individual resting state EEG alpha frequency and cerebral blood flow." Neuroimage **51**(1): 365-372.

Jann, K., M. Kottlow, T. Dierks, C. Boesch and T. Koenig (2010). "Topographic electrophysiological signatures of FMRI Resting State Networks." PLoS One **5**(9): e12945.

Johnstone, T., K. S. Ores Walsh, L. L. Greischar, A. L. Alexander, A. S. Fox, R. J. Davidson and T. R. Oakes (2006). "Motion correction and the use of motion covariates in multiple-subject fMRI analysis." Hum Brain Mapp **27**(10): 779-788.

Kay, S. R., A. Fiszbein and L. A. Opler (1987). "The positive and negative syndrome scale (PANSS) for schizophrenia." Schizophr Bull **13**(2): 261-276.

Klimesch, W. (1997). "EEG-alpha rhythms and memory processes." Int J Psychophysiol **26**(1-3): 319-340.

Koenig, T., D. Lehmann, N. Saito, T. Kuginuki, T. Kinoshita and M. Koukkou (2001). "Decreased functional connectivity of EEG theta-frequency activity in first-episode, neuroleptic-naive patients with schizophrenia: preliminary results." Schizophr Res **50**(1-2): 55-60.

Kottlow, M., K. Jann, T. Dierks and T. Koenig (2012). "Increased phase synchronization during continuous face integration measured simultaneously with EEG and fMRI." Clin Neurophysiol **123**(8): 1536-1548.

Laufs, H., A. Kleinschmidt, A. Beyerle, E. Eger, A. Salek-Haddadi, C. Preibisch and K. Krakow (2003). "EEG-correlated fMRI of human alpha activity." Neuroimage **19**(4): 1463-1476.

Laufs, H., K. Krakow, P. Sterzer, E. Eger, A. Beyerle, A. Salek-Haddadi and A. Kleinschmidt (2003). "Electroencephalographic signatures of attentional and cognitive default modes in spontaneous brain activity fluctuations at rest." Proc Natl Acad Sci U S A **100**(19): 11053-11058.

Lund, T. E., M. D. Norgaard, E. Rostrup, J. B. Rowe and O. B. Paulson (2005). "Motion or activity: their role in intra- and inter-subject variation in fMRI." Neuroimage **26**(3): 960-964.

Mantini, D., M. G. Perrucci, C. Del Gratta, G. L. Romani and M. Corbetta (2007). "Electrophysiological signatures of resting state networks in the human brain." Proc Natl Acad Sci U S A **104**(32): 13170-13175.

McNally, J. M. and R. W. McCarley (2016). "Gamma band oscillations: a key to understanding schizophrenia symptoms and neural circuit abnormalities." Curr Opin Psychiatry **29**(3): 202-210.

Moosmann, M., P. Ritter, I. Krastel, A. Brink, S. Thees, F. Blankenburg, B. Taskin, H. Obrig and A. Villringer (2003). "Correlates of alpha rhythm in functional magnetic resonance imaging and near infrared spectroscopy." Neuroimage **20**(1): 145-158.

Pettersson-Yeo, W., P. Allen, S. Benetti, P. McGuire and A. Mechelli (2011). "Dysconnectivity in schizophrenia: where are we now?" Neurosci Biobehav Rev **35**(5): 1110-1124.

Richard Clark, C., M. D. Veltmeyer, R. J. Hamilton, E. Simms, R. Paul, D. Hermens and E. Gordon (2004). "Spontaneous alpha peak frequency predicts working memory performance across the age span." Int J Psychophysiol **53**(1): 1-9.

Scheeringa, R., K. M. Petersson, A. Kleinschmidt, O. Jensen and M. C. Bastiaansen (2012). "EEG alpha power modulation of fMRI resting-state connectivity." Brain Connect **2**(5): 254-264.

Siekmeier, P. J. and S. M. Stufflebeam (2010). "Patterns of spontaneous magnetoencephalographic activity in patients with schizophrenia." J Clin Neurophysiol **27**(3): 179-190.

Singer, W. (1999). "Neuronal synchrony: a versatile code for the definition of relations?" Neuron **24**(1): 49-65, 111-125.

Singer, W. (2001). "Consciousness and the binding problem." Ann N Y Acad Sci **929**: 123-146.

Stephan, K. E., K. J. Friston and C. D. Frith (2009). "Dysconnection in schizophrenia: from abnormal synaptic plasticity to failures of self-monitoring." Schizophr Bull **35**(3): 509-527.

Toscani, M., T. Marzi, S. Righi, M. P. Viggiano and S. Baldassi (2010). "Alpha waves: a neural signature of visual suppression." Exp Brain Res **207**(3-4): 213-219.

Tyvaert, L., P. Levan, C. Grova, F. Dubeau and J. Gotman (2008). "Effects of fluctuating physiological rhythms during prolonged EEG-fMRI studies." Clin Neurophysiol **119**(12): 2762-2774.

Uhlhaas, P. J. (2011). "High-frequency oscillations in schizophrenia." Clin EEG Neurosci **42**(2): 77-82.

Uhlhaas, P. J., C. Haenschel, D. Nikolic and W. Singer (2008). "The role of oscillations and synchrony in cortical networks and their putative relevance for the pathophysiology of schizophrenia." Schizophr Bull **34**(5): 927-943.

Uhlhaas, P. J. and W. Singer (2006). "Neural synchrony in brain disorders: relevance for cognitive dysfunctions and pathophysiology." Neuron **52**(1): 155-168.

Uhlhaas, P. J. and W. Singer (2010). "Abnormal neural oscillations and synchrony in schizophrenia." Nat Rev Neurosci **11**(2): 100-113.

Van Dijk, K. R., M. R. Sabuncu and R. L. Buckner (2012). "The influence of head motion on intrinsic functional connectivity MRI." Neuroimage **59**(1): 431-438.

Whitfield-Gabrieli, S. and J. M. Ford (2012). "Default mode network activity and connectivity in psychopathology." Annu Rev Clin Psychol **8**: 49-76.

Wood, G., H. C. Nuerk, D. Sturm and K. Willmes (2008). "Using parametric regressors to disentangle properties of multi-feature processes." Behav Brain Funct **4**: 38.

Wu, L., T. Eichele and V. D. Calhoun (2010). "Reactivity of hemodynamic responses and functional connectivity to different states of alpha synchrony: a concurrent EEG-fMRI study." Neuroimage **52**(4): 1252-1260.

Zhang, S. and C. S. Li (2012). "Functional connectivity mapping of the human precuneus by resting state fMRI." Neuroimage **59**(4): 3548-3562.

		San Francisco V.A. Medical Center				University of Bern, Switzerland				Both sites				
		HC (N = 20)		PP (N = 25)		HC (N = 17)		PP (N = 17)		HC (N = 37)		PP (N = 42)		Group difference
Demographics		*Mean*	*SD*	*Mean*	*SD*	*Mean*	*SD*	*Mean*	*SD*	*Mean*	*SD*	*Mean*	*SD*	*ANOVA*
	Age (years)	37.2	14.2	42.3	13.1	31.5	7.2	34.3	8.4	34.6	11,7	39.1	12.0	F (1.9) p = .168
	Education (years)	15.9	2.3	14.0	2.0	15.4	2.1	12.2	2.6	15.6	2.2	13.2	2.4	F (21.7) p < **0.001**
	Sex (M / F)	16 / 4		23 / 2		13 / 4		14 / 3		29 / 8		37 / 5		
	Handedness (R / L / A)	18 / 1 / 1		23 / 1 / 1		17		17		35 / 1 / 1		40 / 1 / 1		
														Site differences
fMRI		*Mean*	*SD*	*Mean*	*SD*	*Mean*	*SD*	*Mean*	*SD*	*Mean*	*SD*	*Mean*	*SD*	*ANOVA*
	Mean head displacement (mm)	0.08	0.05	0.11	0.06	0.04	0.12	0.049	0.035	0.06	0.04	0.08	0.06	F (4.119) p = **.046**
Clinical data	**CPZE (mg)**			362.4	281.9			329.2	174.3			346.8	234.6	F (.166) p = .687
	PANSS positive			17.8	5.8			13.3	4.8			16.0	5.8	F (7.119) p = **.011**
	PANSS negative			18.7	6.3			13.0	7.7			16.4	7.4	F (6.825) p = **.013**
	PANSS general			32.8	8.2			27.5	12.9			30.7	10.5	F (2.647) p = .112
	PANSS total			69.3	15.0			53.8	22.6			63.0	19.6	F (7.133) p = **.011**

Table 1

Table 1: Demographic, clinical and movement information of subjects from each measuring site separately and merged for healthy controls (HC) and psychotic patients (PP). Sex (M= male, F = female); Handedness (R = right-handed, L = left-handed, A = ambidextrous), CPZE = Chlorpromazine equivalence dosage, PANSS = Positive and negative syndrome scale

			Measuring site	
			SFVAMC	**PUK Bern**
EEG	**Acquisition parameters**	**# channels**	32	92
		Reference / ground electrodes	FCz / AFz	Fz / AFF2
		Online bandpass filter	0.01 – 250Hz	0.1 – 250Hz
	Preprocessing	**MR gradient artifact**	Template subtraction (sliding window: 21)	
		Down-sampling	250Hz	500Hz
		Heart beat detection	Filter ECG channel (1-20Hz)	x
		Cardio ballistic artifact	Template subtraction (sliding window: 21)	
		Filters	x	Bandpass 1-49Hz, Notch filter
		Segmentation	2s-epochs on TR, export to Matlab	x
		Removal of electromyography	Canonical correlation analysis (CCA) in Matlab	x
		Reference	Average reference	
		ICA	EEGLAB: 32 components	Vision Analyzer: 64 components
		Remaining artifacts	single-epoch, single-channel artifacts were flagged with FASTER	Manually marked as bad intervals
		Interpolation	Flagged artifacts: EEGLAB spherical spline interpolation function in Matlab	Bad channels: Spherical spline interpolation
fMRI	**Acquisition parameters**	**Scanner**	3T Siemens Skyra	3T Siemens Magnetom Trio
		EPI Sequenzen	TR = 2000ms, TE = 30ms, flip angle = 77°, 30 slices in ascending order, 3.4x3.4x4.0mm voxel size, 182 frames, 6:08 min	TR = 1960ms, TE = 30ms, flip angle = 90°, 35 slices in interleaved order, 3x3x3mm voxel size, 250 frames, 8:17 min

		T1	TR = 2300ms, TE = 2.98ms, flip angle = 9°, 176 sagittal slices, 1x1x1.2mm voxel size, 1.2mm slice thickness	TR = 2300ms, TE = 2.98ms, flip angle: 9°, 176 sagittal slices, 1x1x1mm voxel size, 1.0mm slice thickness
	Preprocessing	**SPM8**	Realignment to mean image	Slice time correction
			Slice time correction	Realignment to mean image
			Co-registration of T1 to the mean image	
			Segmentation into 6 tissue probability maps	
			Normalization and smoothing using a Gaussian FHWH kernel (6x6x6mm)	

Table 2

Table 2: EEG and fMRI acquisition parameters and preprocessing for each measuring site. EPI = Echo planar imaging; TR = Repetition time; TE = Echo time

Formula 1: Computation of EEG Global Field Synchronization (GFS) according to Koenig et al. (2001). E (f) 1 and E (f) 2 are the eigenvalues 1 and 2 obtained from the PCA

Figure captions:

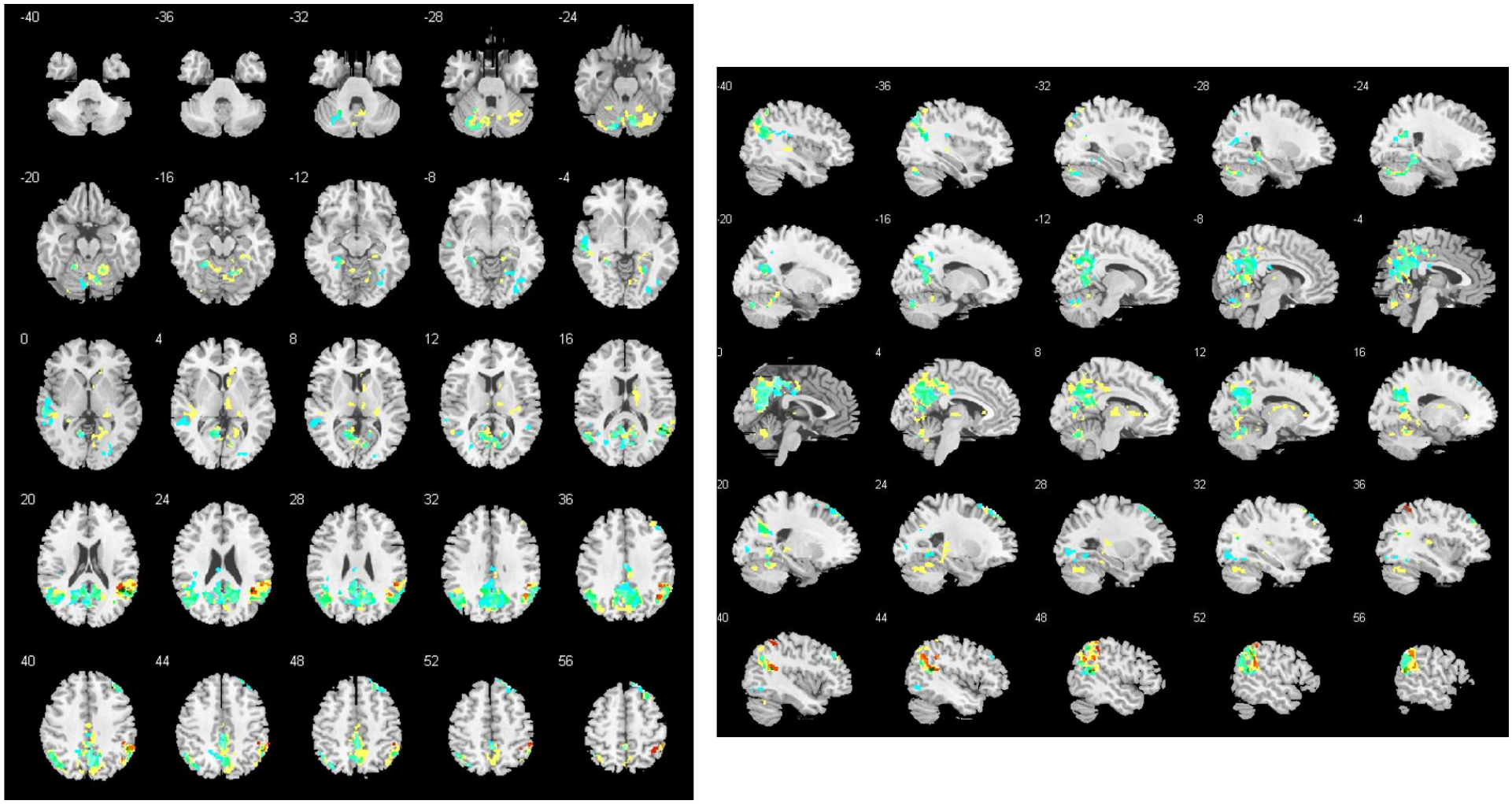

Figure 1: GFS Delta band: a) Horizontal b) sagittal view of significant negative clusters between groups (PP – HC, yellow), positive clusters in HC (red) and negative clusters in PP (light blue; initial threshold p = 0.01, two-sided)

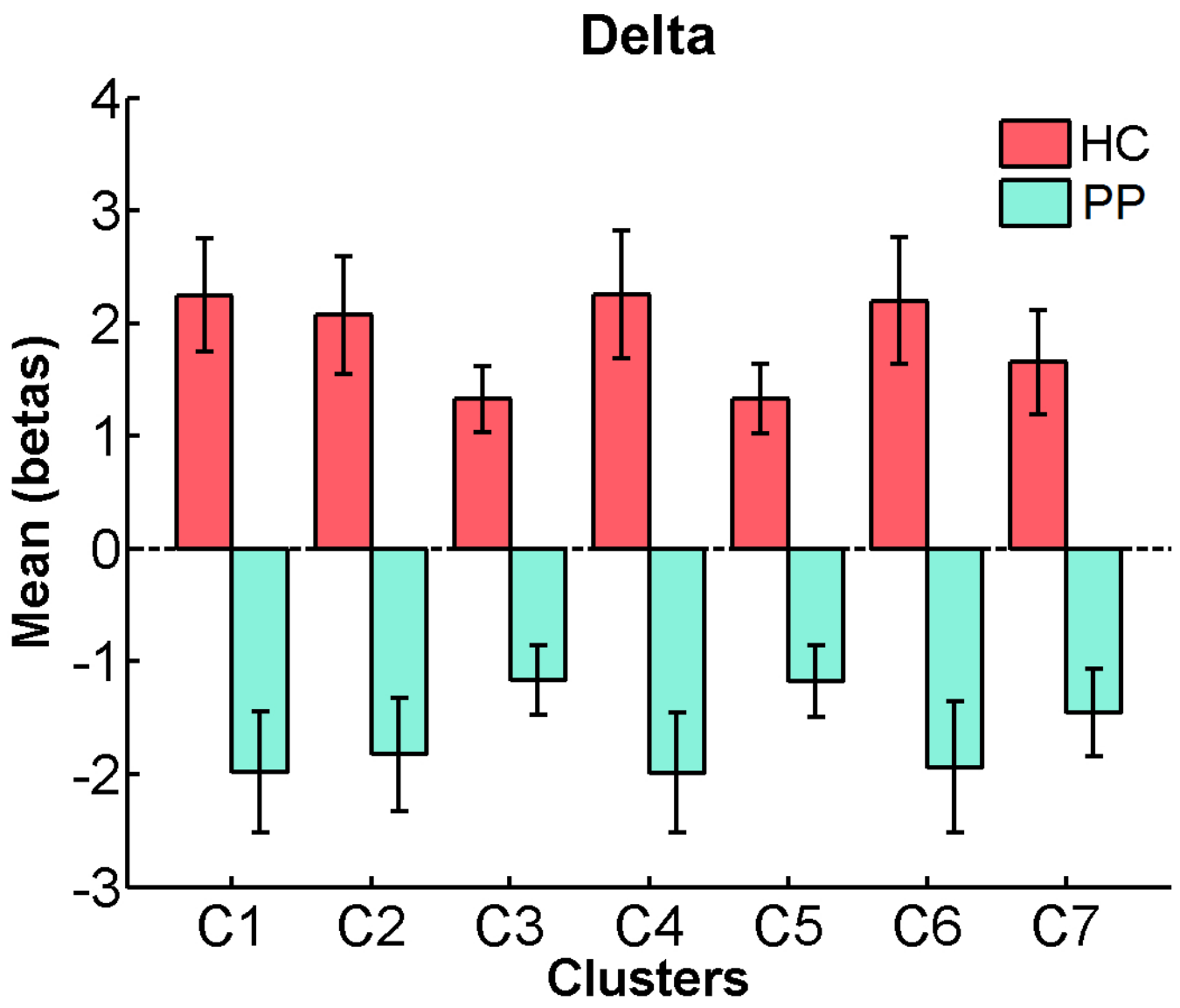

Figure 2: Mean beta weights and standard errors (SE) of significant Delta band clusters for each group

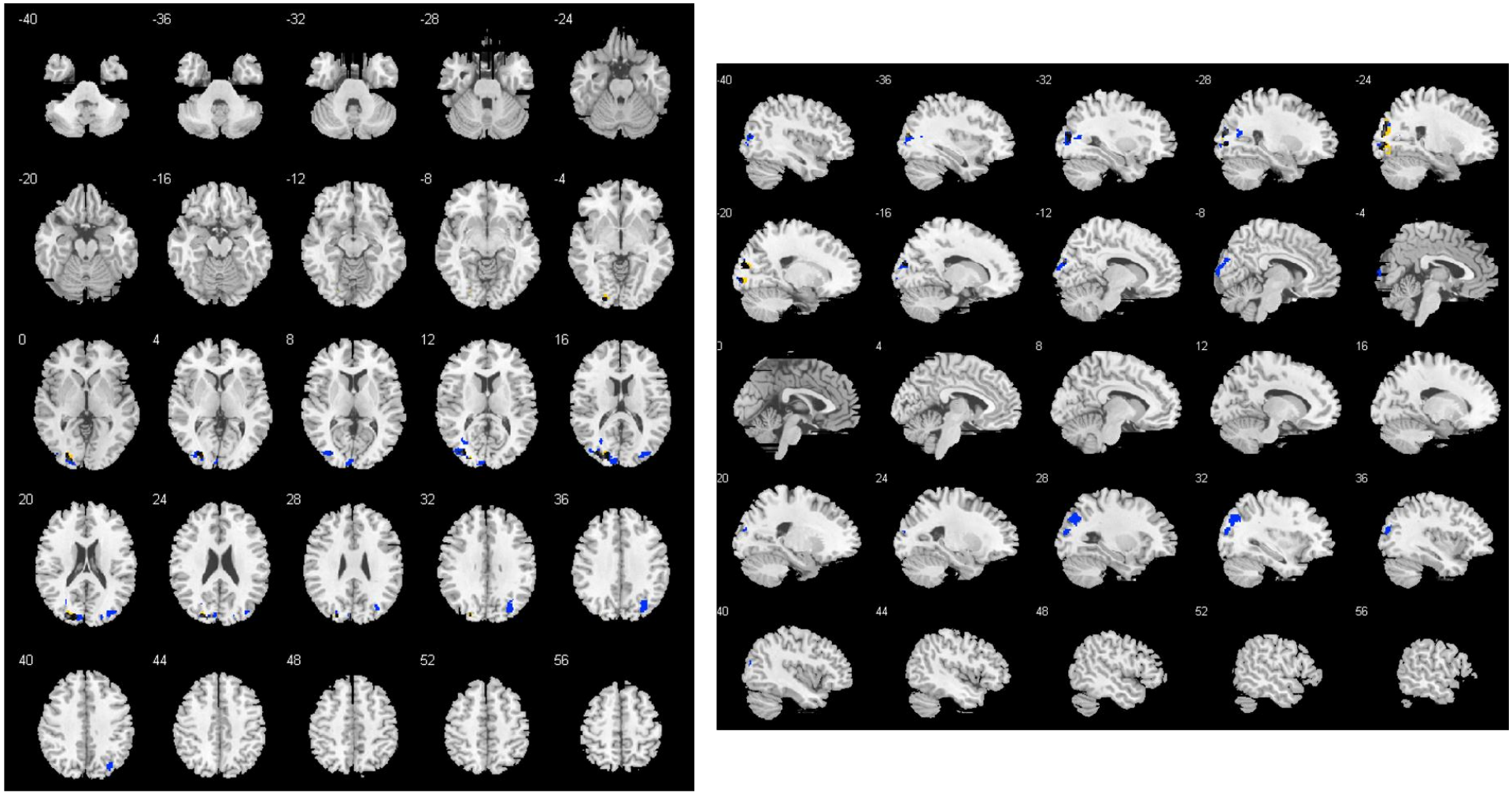

Figure 3: GFS Alpha1 band: a) Horizontal b) sagittal view of significant negative cluster between groups (PP – HC, yellow) and negative clusters in HC (dark blue; initial threshold p = 0.01, two-sided)

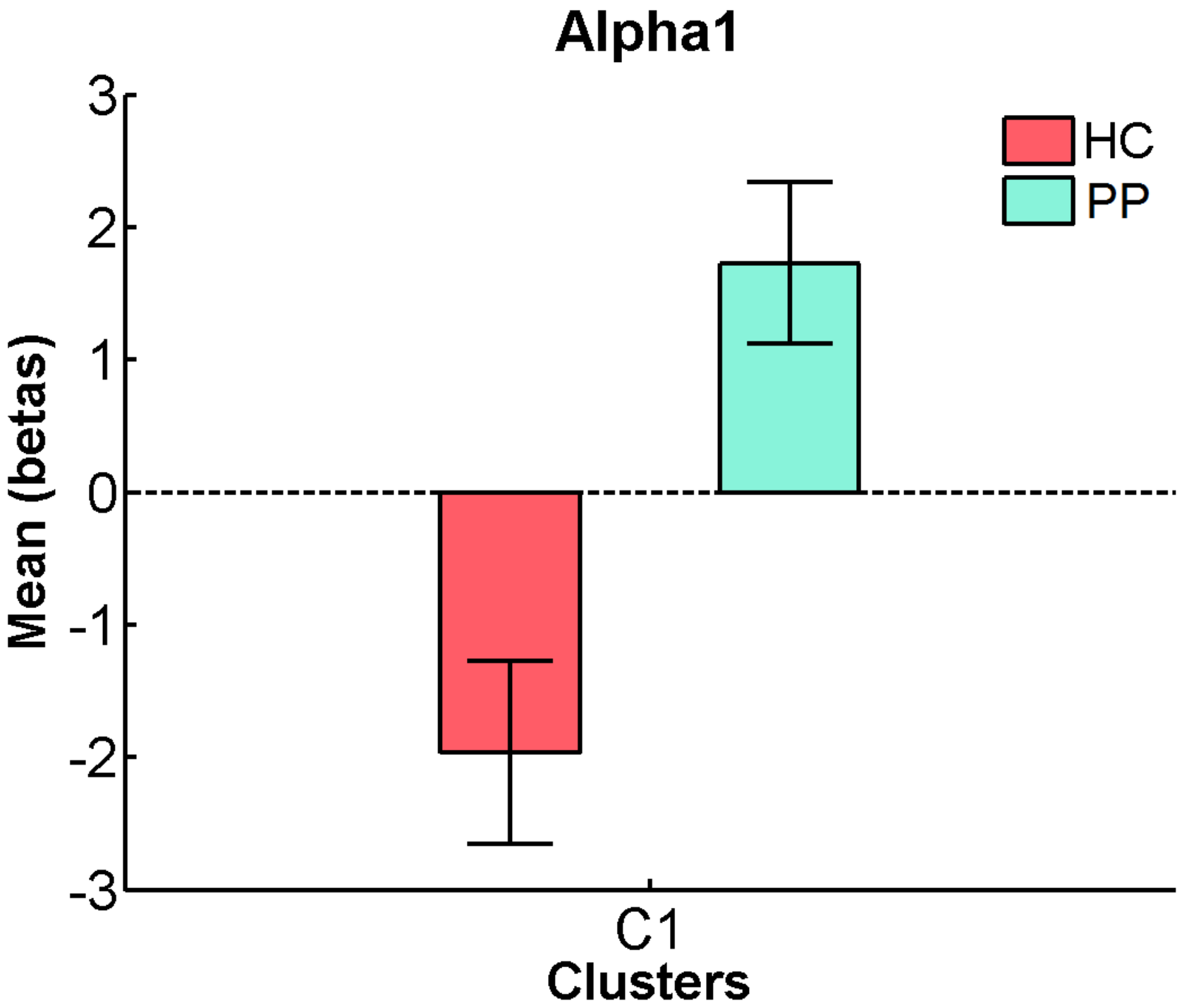

Figure 4: Mean beta weights and standard errors (SE) of significant Alpha1 band cluster for each group

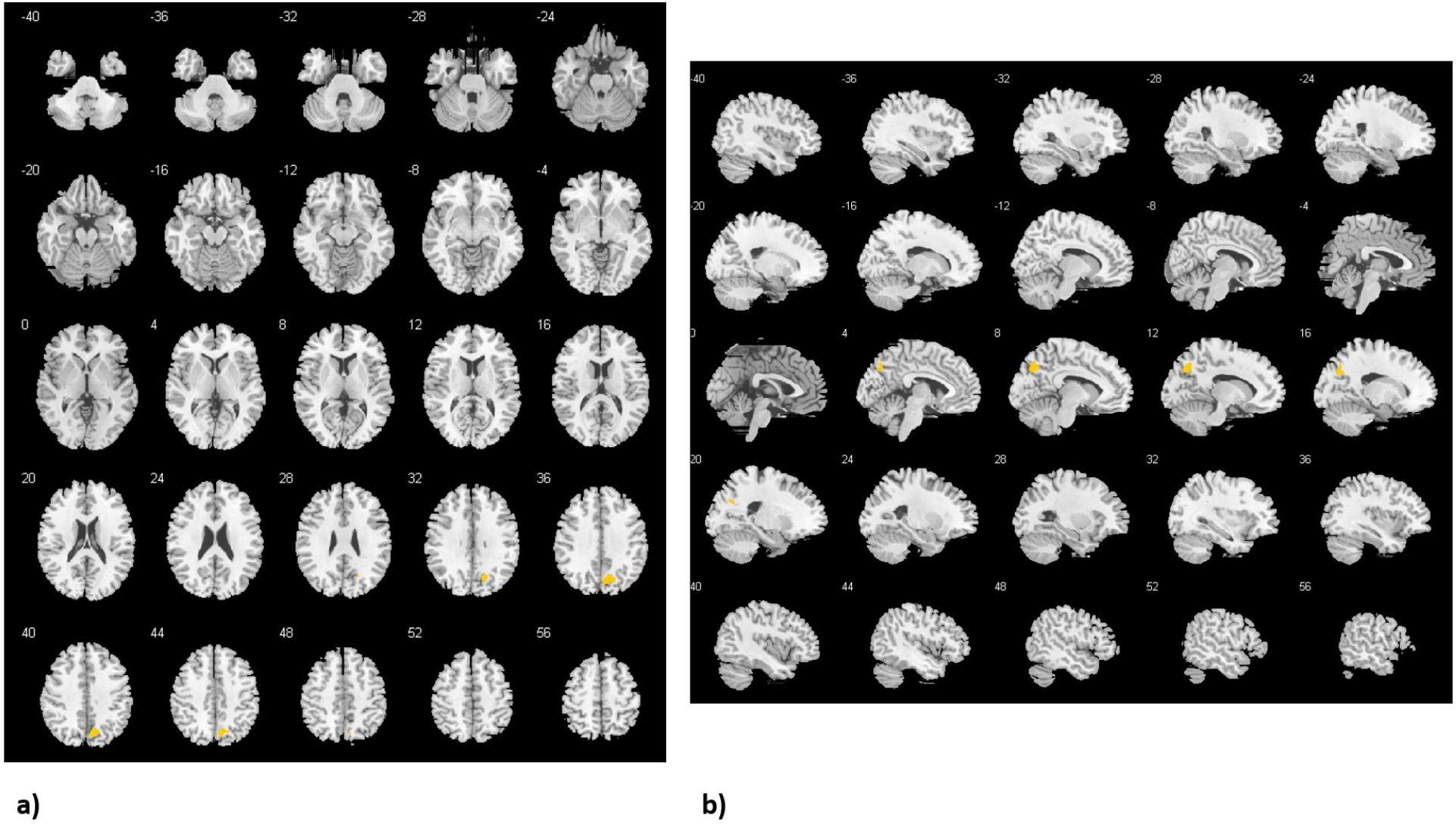

Figure 5: GFS Beta band: a) Horizontal b) sagittal view of significant positive cluster between groups (PP – HC, initial threshold p = 0.01, two-sided)

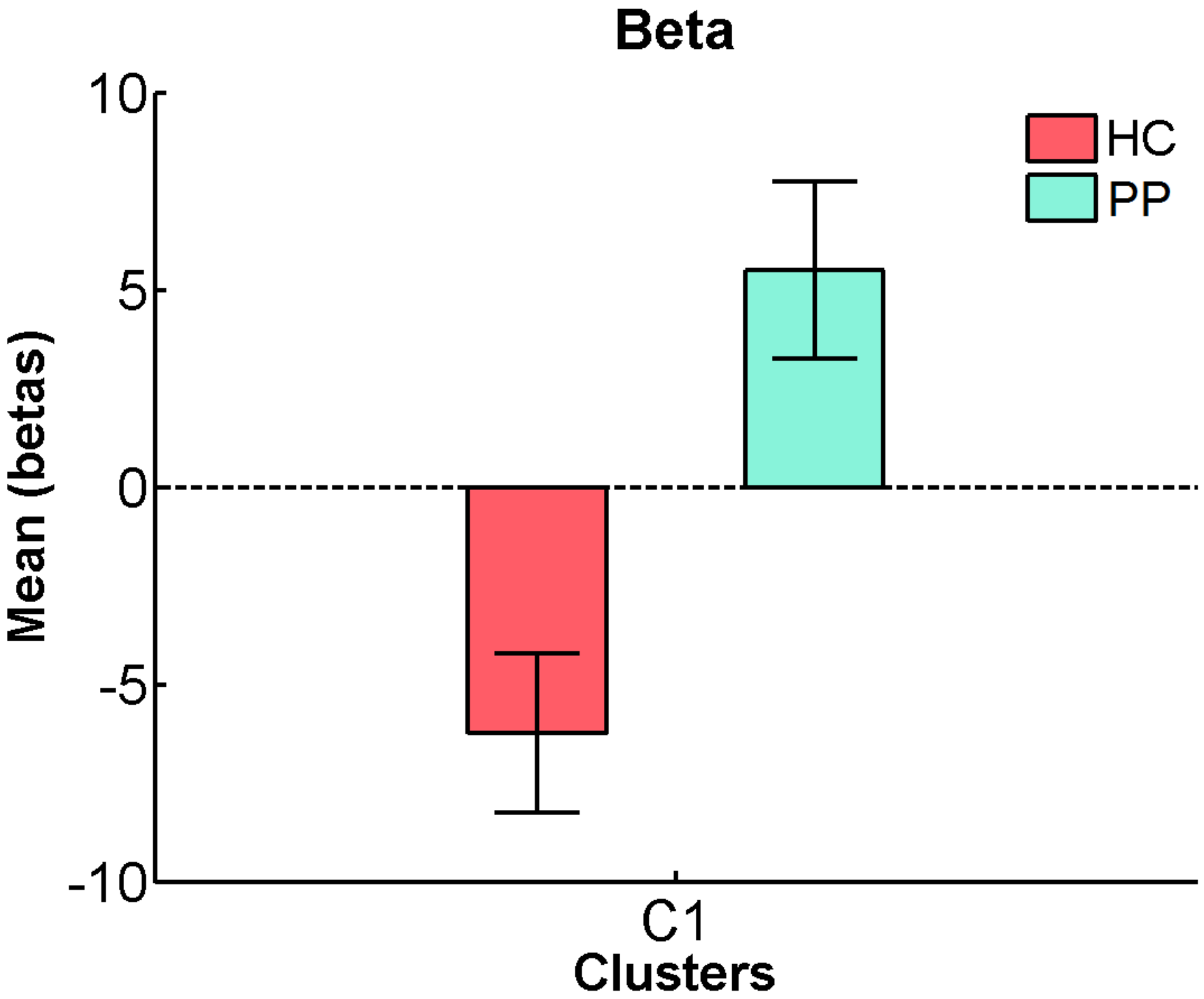

Figure 6: Mean beta weights and standard errors (SE) of significant Beta band cluster for each group

$$GFS(f) = \frac{|E(f)_1 - E(f)_2|}{E(f)_1 + E(f)_2}$$

Formula 1

Supplemental materials:

DELTA (1 – 3.5Hz)

Cluster 1 5506 voxels Peak intensity: 1		Cluster 2 1762 voxels Peak intensity: 1		Cluster 3 1420 voxels Peak intensity: 1		Cluster 4 308 voxels Peak intensity: 1		Cluster 5 293 voxels Peak intensity: 1		Cluster 6 232 voxels Peak intensity: 1		Cluster 7 220 voxels Peak intensity: 1	
# voxels (≥ 10)	structure	# voxels (≥ 10)	structure	# voxels (≥ 10)	structure	# voxels (≥ 10)	structure	# voxels (≥ 10)	structure	# voxels (≥ 10)	structure	# voxels (≥ 10)	structure
2196	Right Cerebrum	1761	Right Cerebrum	1401	Left Cerebrum	286	Right Cerebrum	293	Left Cerebrum	226	Frontal Lobe	208	Right Cerebrum
1917	Left Cerebrum	1194	White Matter	865	White Matter	218	Gray Matter	279	Temporal Lobe	226	Right Cerebrum	114	White Matter
1882	Precuneus	1103	Parietal Lobe	825	Parietal Lobe	132	Thalamus	176	Temporal Mid L	175	Superior Frontal G	83	Gray Matter
1839	White Matter	632	Inferior Parietal L	672	Angular L	114	Thalamus R	169	White Matter	134	Frontal Sup R	66	Limbic Lobe
1774	Parietal Lobe	614	Temporal Lobe	563	Temporal Lobe	97	Caudate R	157	Sup. Temporal G	115	Gray Matter	62	Parahippocampal G
1600	Gray Matter	576	Angular R	491	Gray Matter	86	Caudate	112	Gray Matter	87	White Matter	41	Thalamus
1391	Limbic Lobe	498	Gray Matter	330	Inferior Parietal L	80	White Matter	85	Mid. Temporal G	85	Frontal Mid R	38	Parahhippocampal R
1169	Precuneus R	392	Supramarginal G	283	Temporal Mid L	72	Medial Dorsal N	67	Temporal Sup L	81	Brodmann area 8	32	Pulvinar
853	Cerebellum Post Lobe	385	Superior Temporal G	262	Sup. Temporal G	49	Caudate Body	54	Brodmann area 21	51	Middle Frontal G	29	Hippocampus R
850	Precuneus L	307	SupraMarginal R	246	Middle Temporal G	37	Caudate Head	33	Brodmann area 22	27	Brodmann area 9	26	Insula
832	Declive	306	Brodmann area 40	233	Brodmann area 39	30	Corpus Callosum	10	Insula			22	Fusiform R
800	Posterior Cingulate	292	Parietal Inf R	202	Supramarginal G	22	Thalamus L					15	Thalamus R
712	Right Cerebellum	206	Temporal Mid R	198	Parietal Inf L	20	Left Cerebrum					14	Brodmann area 13
628	Brodmann area 7	183	Temporal Sup R	194	Angular G	19	Ventral Lateral N					14	Insula R
604	Occipital Lobe	124	Angular Gyrus	127	Brodmann area 40							11	Heschl R
534	Left Cerebellum	106	Middle Temporal G	120	Occipital Mid L							10	Culmen
499	Cingulate Gyrus	105	Brodmann area 39	91	Precuneus							10	Cerebellum Anter. L
494	Brodmann area 31	53	Brodmann area 13	63	Sup. Parietal L							10	Temporal Lobe
415	Cerebelum 6 R	42	Insula	59	Brodmann area 7							10	Right Cerebellum
393	Cerebellum Anterior L	40	Occipital Mid R	51	SupraMarginal L								
365	Culmen	21	Brodmann area 7	51	Brodmann area 19								
308	Calcarine L	14	Parietal Sup R	35	Parietal Sup L								
254	Cingulum Mid L	13	Sup Parietal Lobule	21	Brodmann area 22								
248	Cerebelum Crus1 L	13	Brodmann area 22	17	Temporal Sup L								
228	Cingulum Mid R			13	Occipital Lobe								
222	Cuneus L												
206	Lingual R												
203	Cuneus R												
176	Calcarine R												
172	Cingulum Post L												
169	Cuneus												
167	Lingual Gyrus												
163	Frontal Lobe												
160	Paracentral L												
131	Brodmann area 30												
120	Brodmann area 23												
112	Cerebelum 6 L												
107	Cerebelum 4/5 R												
106	Temporal Lobe												
94	Parahippocampa G												
91	Cerebelum 4/5 L												
91	Vermis 6												
88	Lingual L												
74	Cingulum Post R												
63	Brodmann area 18												
62	Fusiform L												
45	Brodmann area 5												
40	Cerebelum Crus1 R												
32	Occipital Sup L												
32	Vermis 7												
31	Parahippocampal L												
27	Brodmann area 29												
26	Brodmann area 19												

25	Hippocampus L						
24	Vermis 4/5						
24	Brodmann area 24						
19	Occipital Sup R						
19	Fusiform Gyrus						
18	Vermis 8						
15	Hippocampus						
14	Nodule						
13	Corpus Callosum						
12	Declive of Vermis						
12	Brodmann area 36						
12	Brodmann area 37						
11	Cerebelum Crus 2 L						

Table 1: Significant between-group clusters in GFS delta, alpha1 and beta band

Detailed procedure for EEG preprocessing at both sites:

SFVAMC:

1. Correction for MR gradient artifacts using artifact subtraction proposed by Allen et al. (Allen, Josephs et al. 2000) as implemented in Brain Vision Analyzer. The correction involved subtracting an artifact template from the raw data, using a baseline-corrected sliding average of 21 consecutive volumes to generate the template.
2. Down-sampling of EEG data to 250Hz.
3. Removal of ballistocardiac artifact by subtracting a heartbeat template from the EEG, using a sliding average of 21 (±10 centered on a given pulse) heartbeat events as originally proposed (Allen, Polizzi et al. 1998) and done by others (Schulz, Regenbogen et al. 2015, Shams, Alain et al. 2015). Parameters of the semi-automatic heartbeat detection in Brain Vision Analyzer were: high temporal correlation (r >.5) and above threshold amplitude (0.6-1.7) with trained research assistants adjusting templates, search windows, and manually identifying pulses as needed.
6. Canonical correlation analysis (CCA) was used as a blind source separation technique to remove broadband or electromyography (EMG) noise from single trial data using a method similar to that used by others (De Clercq, Vergult et al. 2006, Ries, Janssen et al. 2013) with some important differences. The CCA de-noising procedure involves correlating time series data from all channels with the one-sample time-lagged series from all channels, which is the multivariate equivalent of auto-regressive time series correlation. Each set of canonical correlation coefficients (one for each electrode resulting in 31 for this study) has an associated time series (i.e., linear function of the coefficients and raw data called canonical variates). The Fast Fourier Transformed (FFT) power spectra of these canonical variate time series have been used to identify EMG components by taking the ratio of high (e.g., 15 to 30Hz) to low (e.g., <15Hz) power and removing components with ratios greater than a pre-determined limit (e.g., if high/low > 1/5 in (Ries, Janssen et al. 2013). This is a very rough heuristic for determining if a canonical variate's power spectrum has Power-law scaling (e.g., $1/f^{\beta}$ or f^{α}, where $-\beta=\alpha$) where log-transformed power decreases linearly with increasing log-transformed frequency. Previous studies (Pereda, Gamundi et al. 1998, Freeman, Holmes et al. 2003) have suggested that the exponent, α, is less than -1 in human EEG, while white noise or EMG would have an exponent of approximately zero. Using simple linear regression, we estimated α by predicting log-power with log-frequency. For each trial and canonical variate, a bootstrap confidence interval was constructed for the estimated α by randomly sampling, without replacement, half of the frequency bins between 1-125Hz from the FFT one thousand times to avoid potential contamination by a few frequencies (i.e., 60Hz or alpha-band). If the interval contained values less than -1, the component was retained while all others were algebraically removed during back-projection to the original EEG epoch space.
7. Single trial data were re-referenced to an average reference, and data were obtained for the prior reference channel, FCz.
8. Outlier trials were rejected based on previously established criteria from FASTER (Nolan, Whelan et al. 2010, Ford, Palzes et al. 2014)
9. Independent components analysis (ICA) was then performed on each subject in EEGLAB (Delorme and Makeig 2004), generating 32 independent components.

10. Noise components were identified by FASTER criteria (Nolan, Whelan et al. 2010), and also spatial correlations of |r|>0.8 with eye blink and ballistocardiac artifact templates. The eyeblink template was created by averaging components resembling frontal-only activity, while the ballistocardiac template was created by setting midline electrodes to 0 and the two hemispheres with opposing signs, resembling a dipole effect (see figure 1). These noise components were then removed from the data during back-projection (in controls: mean = 7.1, SD =2.1; in patients: mean = 8.0, SD = 3.2 out of 32 components).

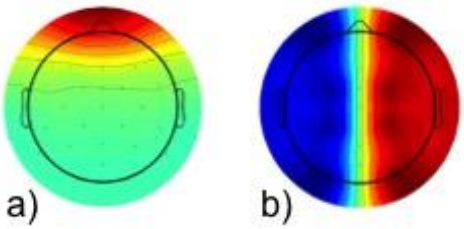

Figure 1: Templates for removal of a) eyeblink and b) ballistocardiac artifacts using FASTER

PUK Bern:

The procedures used for artifact removal are based on previous literature (Jann, Dierks et al. 2009, Jann, Kottlow et al. 2010, Kottlow, Jann et al. 2012, Razavi, Jann et al. 2013, Kottlow, Schlaepfer et al. 2015) and briefly summarized here:

1. By means of average artifact subtraction with a sliding window of 21 (Allen, Josephs et al. 2000), the EEG was corrected for MR related artifacts including scan-pulse and cardio-ballistic artifact.
2. EEG files from outside and inside of the scanner were down-sampled to 500Hz and concatenated.
3. Application of a bandpass filter (1 – 49Hz and a notch filter) to the concatenated file and disabling of bad channels.
4. Further cleaning of the EEG from remaining scan-pulse, cardio-ballistic and eye movement artifacts using an ICA-based approach (number of ICA components removed in controls: mean = 20.5, SD = 2.7; in patients: mean = 18.4, SD = 3.4 out of 64 components). By visual inspection of the components' temporal dynamics, topographic maps, and the comparison of their power spectra from inside versus outside of the scanner, components loading for artifacts were identified. Then, the EEG of each subject was reconstructed from the remaining factors.
5. Manual marking of epochs containing residual scanner or movement artifacts and interpolating of disabled channels using a spherical spline interpolation.
6. After removal of the ECG and EOG channels, the EEG was recalculated to average reference.

References

Allen, P. J., O. Josephs and R. Turner (2000). "A method for removing imaging artifact from continuous EEG recorded during functional MRI." Neuroimage **12**(2): 230-239.

Allen, P. J., G. Polizzi, K. Krakow, D. R. Fish and L. Lemieux (1998). "Identification of EEG events in the MR scanner: the problem of pulse artifact and a method for its subtraction." Neuroimage **8**(3): 229-239.

De Clercq, W., A. Vergult, B. Vanrumste, W. Van Paesschen and S. Van Huffel (2006). "Canonical correlation analysis applied to remove muscle artifacts from the electroencephalogram." IEEE Trans Biomed Eng **53**(12 Pt 1): 2583-2587.

Delorme, A. and S. Makeig (2004). "EEGLAB: an open source toolbox for analysis of single-trial EEG dynamics including independent component analysis." J Neurosci Methods **134**(1): 9-21.

Ford, J. M., V. A. Palzes, B. J. Roach and D. H. Mathalon (2014). "Did I do that? Abnormal predictive processes in schizophrenia when button pressing to deliver a tone." Schizophr Bull **40**(4): 804-812.

Freeman, W. J., M. D. Holmes, B. C. Burke and S. Vanhatalo (2003). "Spatial spectra of scalp EEG and EMG from awake humans." Clin Neurophysiol **114**(6): 1053-1068.

Jann, K., T. Dierks, C. Boesch, M. Kottlow, W. Strik and T. Koenig (2009). "BOLD correlates of EEG alpha phase-locking and the fMRI default mode network." Neuroimage **45**(3): 903-916.

Jann, K., M. Kottlow, T. Dierks, C. Boesch and T. Koenig (2010). "Topographic electrophysiological signatures of FMRI Resting State Networks." PLoS One **5**(9): e12945.

Kottlow, M., K. Jann, T. Dierks and T. Koenig (2012). "Increased phase synchronization during continuous face integration measured simultaneously with EEG and fMRI." Clin Neurophysiol **123**(8): 1536-1548.

Kottlow, M., A. Schlaepfer, A. Baenninger, L. Michels, D. Brandeis and T. Koenig (2015). "Pre-stimulus BOLD-network activation modulates EEG spectral activity during working memory retention." Front Behav Neurosci **9**: 111.

Nolan, H., R. Whelan and R. B. Reilly (2010). "FASTER: Fully Automated Statistical Thresholding for EEG artifact Rejection." J Neurosci Methods **192**(1): 152-162.

Pereda, E., A. Gamundi, R. Rial and J. Gonzalez (1998). "Non-linear behaviour of human EEG: fractal exponent versus correlation dimension in awake and sleep stages." Neurosci Lett **250**(2): 91-94.

Razavi, N., K. Jann, T. Koenig, M. Kottlow, M. Hauf, W. Strik and T. Dierks (2013). "Shifted coupling of EEG driving frequencies and fMRI resting state networks in schizophrenia spectrum disorders." PLoS One **8**(10): e76604.

Ries, S., N. Janssen, B. Burle and F. X. Alario (2013). "Response-locked brain dynamics of word production." PLoS One **8**(3): e58197.

Schulz, M. A., C. Regenbogen, C. Moessnang, I. Neuner, A. Finkelmeyer, U. Habel and T. Kellermann (2015). "On utilizing uncertainty information in template-based EEG-fMRI ballistocardiogram artifact removal." Psychophysiology **52**(6): 857-863.

Shams, N., C. Alain and S. Strother (2015). "Comparison of BCG artifact removal methods for evoked responses in simultaneous EEG-fMRI." J Neurosci Methods **245**: 137-146.